Int J Clin Exp Med 2015;8(8):12172-12181
www.ijcem.com /ISSN:1940-5901/IJCEM0008301

Original Article

Impacts of fluorescent superparamagnetic iron oxide (SPIO)-labeled materials on biological characteristics and osteogenesis of bone marrow mesenchymal stem cells (BMSCs)

Guangping Zhang[1*], Zhenwen Na[1*], Bin Ren[1], Xin Zhao[2], Weixian Liu[1]

[1]Department of Oral and Maxillofacial Surgery, Shengjing Hospital of China Medical University, Shengyang 110004, Liaoning Province, China; [2]Department of Prosthetics, School of Stomatology, China Medical University, Shenyang 110002, Liaoning Province, China. [*]Equal contributors.

Received March 21, 2015; Accepted June 3, 2015; Epub August 15, 2015; Published August 30, 2015

Abstract: The aim of this study was to investigate the impacts of fluorescent superparamagnetic iron oxide particles (Molday ION Rhodamine B, MIRB) on bioactivities and osteogenetic differentiation of rat bone marrow mesenchymal stem cells (BMSCs). The Cell Counting Kit-8 (CCK-8) method was used to detect the proliferation of superparamagnetic iron oxide (SPIO)-labeled BMSCs and observed the distribution of MIRB in cells; real time -polymerase chain reaction (RT-PCR) method was used to analyze the expressions of such osteogenesis-related genes as bone sialoprotein, alkaline phosphatase (ALP), RUNX2, bonemorphogeneticprotein-2 (BMP-2), type 1 collagen (COL-1) and type 3 collagen (COL-3); ALP-Alizarin red staining and poly-biochemical analyzer were used to qualitatively and quantitatively analyze the osteogenetic metabolites. The labeled MIRB particles distributed in the cytoplasm of BMSCs, the diameter of larger particles could be up to several hundred nanometers, and concentrated around the nuclei, the particles far away from the nuclei were smaller, but the labeled-cells' skeletons and adherent morphology did not change significantly; under the concentration of 25 μg Fe/mL of, MIRB did not affect cellular viabilities of BMSCs, but the gene expressions of bone sialoprotein, ALP, RUNX2 and BMP-2 were decreased, and the secretion amount of ALP and osteocalcin were also declined. MIRB would not affect the proliferation and cell structures of BMSCs, but the SPIO particles aggregated and formed larger granules around the nuclei, which might affect the osteogenesis of BMSCs.

Keywords: Bone marrow mesenchymal stem cells, superparamagnetic iron oxide, fluorescent labeling, osteogenetic differentiation

Introduction

The stem cell and biological scaffold-based bone defect repairing treatment is currently a hot research in tissue engineering. As the ideal seed cells for tissue engineering, bone marrow mesenchymal stem cell (BMSC) had the advantages of autologous source, easy isolation and amplification, etc., thus it had broad application prospects in bone defect repairing [1, 2], while the migration and localization of transplanted cells towards target organs depended on reliable cell markers. The most commonly used marking methods were immunofluorescence, magnetic marker and radioactive nuclide marker, etc [3-5]. The radioactive nuclide had such shortcomings as short half-life, could not be used for long-term tracking and ionizing radiation. The fluorescent marker could accurately and directly visualize the positions of labeled stem cells, accurately, sensitively and specifically, while it required the animals to be killed, thus it could not be used in vivo tracking. The superparamagnetic iron oxide (SPIO) was the magnetic resonance imaging (MRI)-marking material that had been clinically applied, having good biocompatibilities and MRI-developing capabilities. In recent years, many scholars had applied SPIO in labelling stem cells, and there existed preliminary studies about its impacts on stem cells' proliferation and differentiation capacities [6-9], which proved the wide pros-

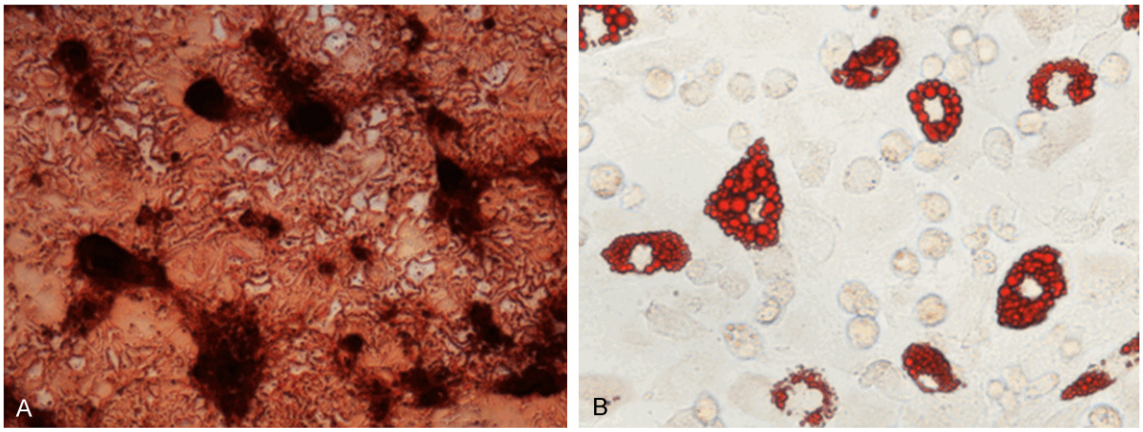

Figure 1. Identification of BMSCs' differentiation. A. Alizarin Red staining, the red-stained Ca nodules could be seen. B. Oil Red O staining, red lipid droplets could be seen in the cytoplasm.

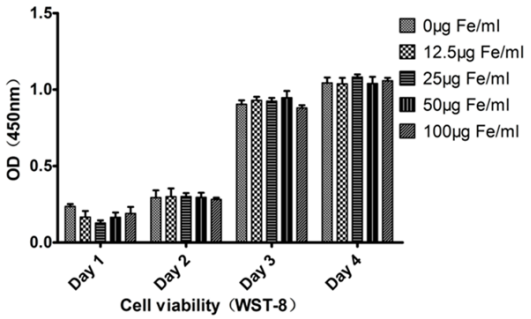

Figure 2. Detection of cellular viability of MIRB-labeled BMSCs. There existed no significant difference in 1st~4th day among all labeling group or compared with the control group (P>0.5).

pects of SPIO in the field of tracking transplanted stem cells. Moreover, with the continuous development of SPIO-labeled materials, the applications of ultra-small SPIO particles (USPIO) and dextran-coating enabled SPIO higher cell-marking rate and longer effective marking time [10, 11].

Stem cell transplantation therapy of bone defects required the implanted BMSC to migrate and rebuild in the injury sites, and converse to the osteoblasts, thus playing the therapeutic roles. This required the SPIO-labeled material did not interfere the normal migration and differentiation of BMSC. After SPIO labelling, it would be very necessary to study the skeleton structures, proliferation, adhesion and differentiation of BMSCs.

In this study, Molday ION Rhodamine B (MIRB) USPIO particles (Biopal Co.) were used, which had double labeling characteristics of MRI and immunofluorescence [10], previous studies reported that the SPIO particles might be phagocytized by macrophages with the splitting and death of labeled cells, thus forming false positive results in MRI developing [4, 8, 12], and the fluorescence-labeled SPIO could easily be located and tracked by fluorescence microscopy, and confirmed each other with MRI images, thus it was one more ideal SPIO-labeled material [13].

In this study, a variety of methods were performed to observe and analyze the distribution of fluorescent SPIO particles in mesenchymal stem cells, as well as the changes of structural phenotypes inside and outside of cells. Meanwhile, the cells' proliferation, osteogenesis-related genes and metabolites were qualitatively and quantitatively analyzed, aiming to establish theoretical basis for future application of SPIO in stem cell bone defect repairing.

Materials and methods

Separation and extraction of BMSCs

SD rats, aged 4-6 weeks old, were selected for the BMSCs extraction by whole bone marrow wall-adherence method, BMSCs were then seeded in 25 cm^2 flasks and cultured with DMEM/F12 (1:1) containing 10% fetal bovine serum (Hyclone, Logan, UT, USA) at 37°C, 5% CO_2 and saturated humidity. The culture medium was firstly changed 48 h later, the passage could be performed when the cells reached 90% fusion. The BMSCs extraction of fluores-

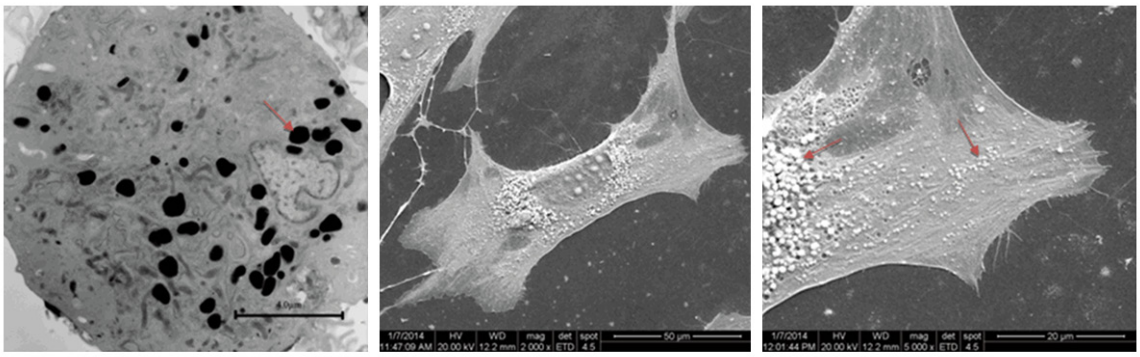

Figure 3. Ultra-structural observation of MIRB-labelled BMSCs. TEM microscopy (3000-time) showed the black SPIO particles distributed in the cytoplasm near the nuclei and the smooth endoplasmic reticulum. SEM showed that the cells were fusiform, the cytoskeletal structures were clear. High-powered microscopy showed that the cells crawled and adhered wall with pseudopodia. Most SPIO particles distributed around the nuclei, the perinuclear particles were as large as up to several hundred nanometers, while those in the cytoplasm far away from nuclei were relatively smaller.

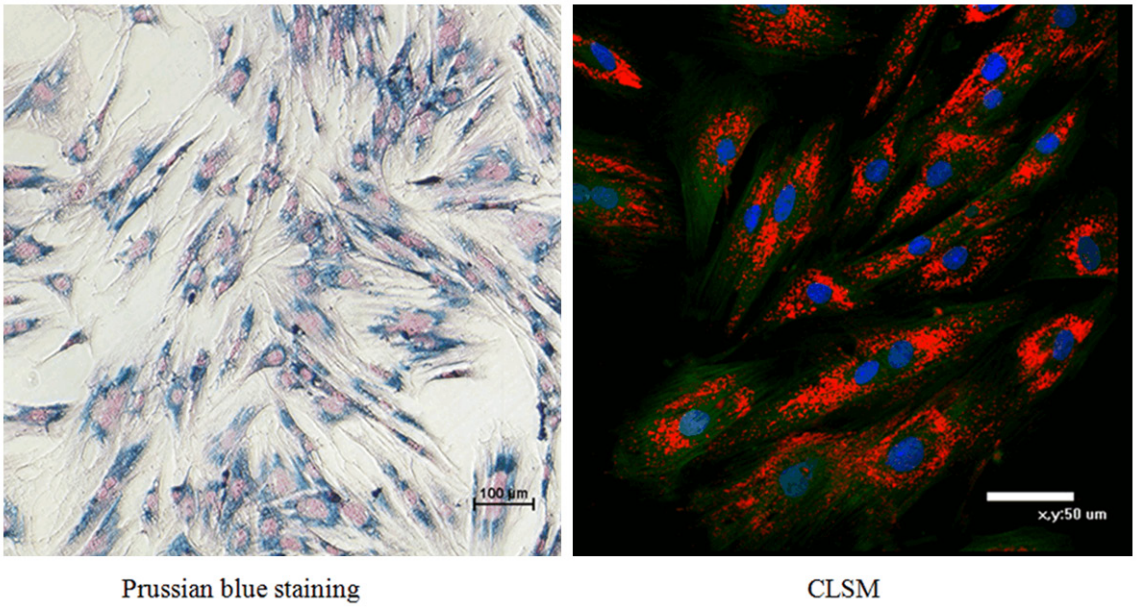

Figure 4. MIRB-labeled Prussian blue staining and confocal microscopic rhodamine fluorescence observation. 100-time microscopy showed that the cytoplasm was feosin-stained, and the SPIO particles were blue-stained. 400-time confocal fluorescence microscopy showed that the green was the green fluorescent protein expressed by the fluorescence-transgenic rats, the red was the fluorescent SPIO particles, and the blue was the DAPI nuclear dye.

cence-transgenic rats was as the above. This study was carried out in strict accordance with the recommendations in the Guide for the Care and Use of Laboratory Animals of the National Institutes of Health. The animal use protocol has been reviewed and approved by the Institutional Animal Care and Use Committee (IACUC) of China Medical University.

Identification by flow cytometry: selected the 4th-generation cells + BMSCs surface antigens were characterized by flow cytometry using fluorescein isothiocyanate-conjugated mouse anti-rat cluster of differentiation (CD)11b and CD45 and phycoerythrin-conjugated mouse anti-rat CD90 and CD29 antibodies (Biolegend, SanDiego, CA, USA). Induction of adipogenic

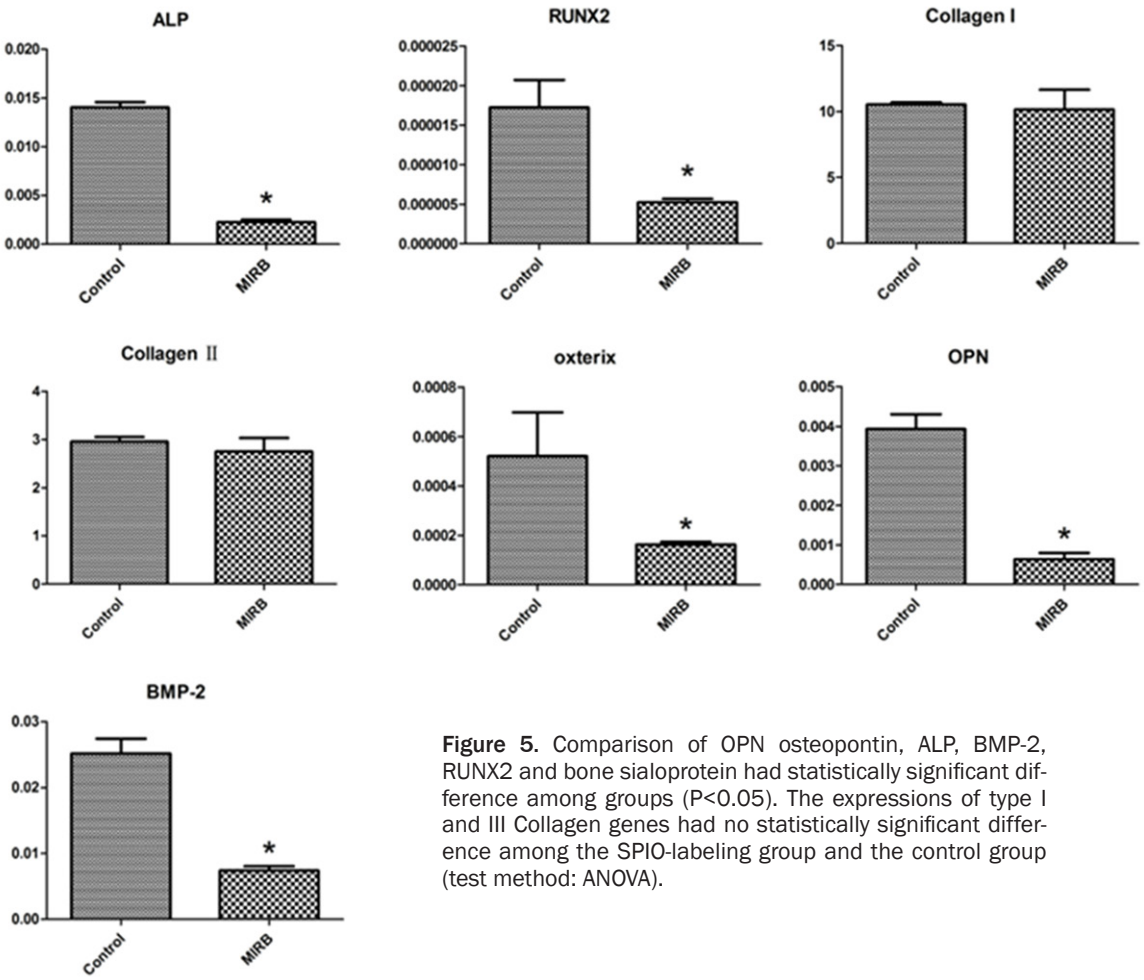

Figure 5. Comparison of OPN osteopontin, ALP, BMP-2, RUNX2 and bone sialoprotein had statistically significant difference among groups ($P<0.05$). The expressions of type I and III Collagen genes had no statistically significant difference among the SPIO-labeling group and the control group (test method: ANOVA).

differentiation: cells from the fourth passage were seeded in 6-well plates at a density of 1×10^4 cells/cm^2 and cultured to 90% confluence with the growth medium, then replace media with pre-warmed Adipogenesis Differentiation Medium (Gibco adipogenic differentiation kit, Grand Island, NY, USA) and continue incubation. MSCs will continue to undergo limited expansion as they differentiate under adipogenic conditions. Refeed cultures every 3 to 4 days, and Oil Red O staining (Sigma, St. Louis, MO, USA) was performed for the identification 8 days later. Osteogenesis-induced differentiation: cells from the fourth passage were seeded in 6-well plates at a density of 5×10^3 cells/cm^2 and cultured to 70% confluence with the growth medium. Then, the medium was changed to osteogenic medium (Gibco osteogenetic differentiation kit, Grand Island, NY, USA). MSCs will continue to expand as they differentiate under osteogenic conditions. Refeed cultures every 3 to 4 days and the cellular Alizarin Red staining (Sigma, St. Louis, MO, USA) was performed 21 days later to detect Ca nodules.

SPIO-labeling

SPIO-labeled solution (Molday ION Rhodamine B, BioPAL Co., Worcester, MA, USA): used DMEM/F12 (1:1) serum-free culture medium to dilute the original USPIO solution (2 mg Fe/mL), adjusted the final concentration of SPIO as (12.5, 25, 50, 100) μg Fe/mL; took the 4th-generation BMSCs for 18 h SPIO-labeling (used equal volume of SPIO-labeling liquid to replace the culture medium), discarded the labeling fluid 18 h later, and the Prussian blue staining was performed to detect the intracellular SPIO distribution.

Detection of cell proliferation

The purified 4th-generation cells were grouped and labeled according to the SPIO-labeling method described above with the SPIO concen-

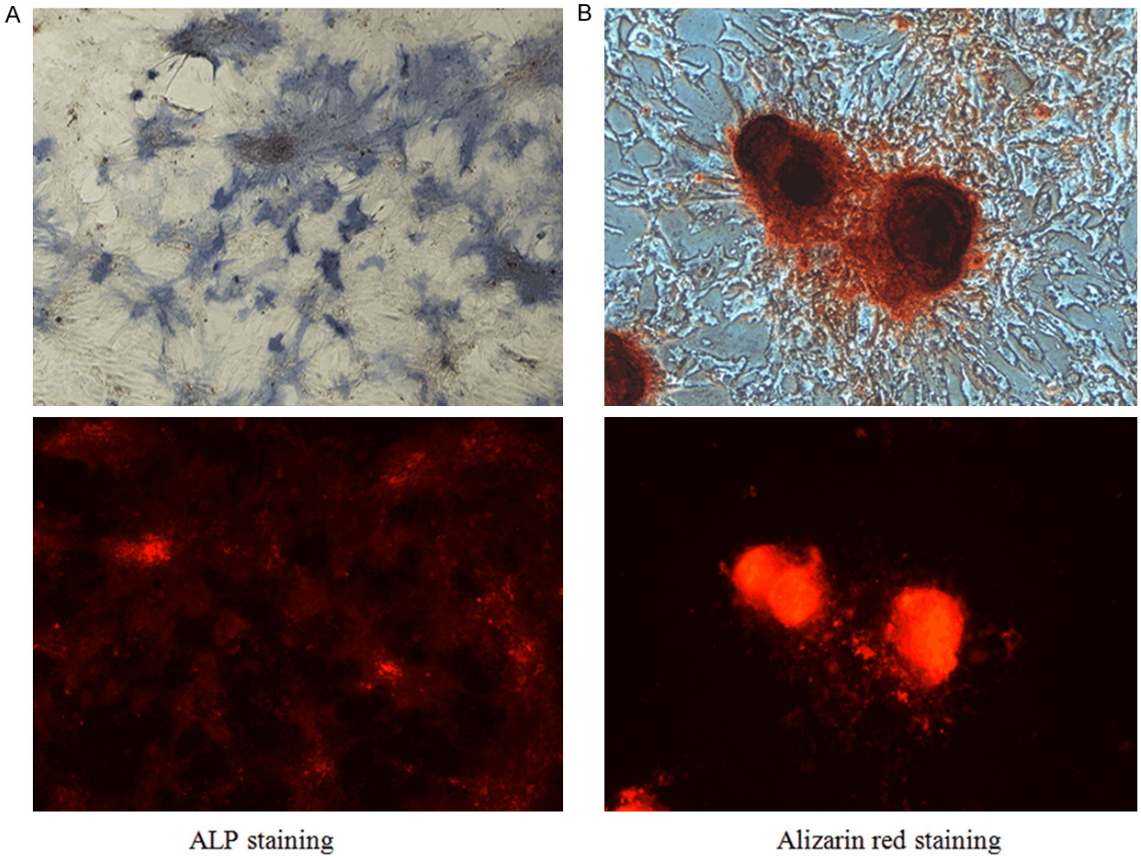

Figure 6. Detection of osteogenesis of MIRB-labeled BMSCs. A. Under the fluorescence microscope, ALP-positive staining area and correspondingfluorescent SPIO distribution area. B. 21 days after osteogenetic induction, the Alizarin Red staining method stained the Ca nodules and the corresponding fluorescent SPIO imaging.

trations as 0, 12.5, 25, 50 and 100 μg Fe/mL, then the automatic ELISA analyzer, with Cell Counting Kit-8 (CCK-8) (Beyotime Co., Shanghai, China), was used to record the OD absorbance values of different concentration groups on the 1st-4th day at 450 nm wavelength, and the growth curves were then drawn.

Morphologic and structural observation of SPIO-labeled cells

Scanning electron microscope (SEM): the 25 μg Fe/mL group was used for the cellular morphologic and structural observation. The labeled cells were inoculated in a glass culture dish, when the cells were wall-adherent, rinsed with PBS, fixed with glutaraldehyde for 2 h, rinsed with PBS, fixed with 1% osmic acid for 2 h, dehydrated with acetone, dried ay critical point, then performed gold sputtering by ion spraying method for 2 min. After the SEM specimens were prepared, the cell morphology was observed by FEI QUANT 600 SEM, and the elemental compositions were analyzed using spectral analysis. Transmission electron microscope (TEM): digested and separated another part of BMSCs of SPIO-labeling group and control group, centrifuged and discarded the supernatant, then used glutaraldehyde to prepare the TEM specimens, the FEI TECNAI G2 TEM was then used to observe the BMSCs samples, and the elemental compositions were analyzed using spectral analysis. Laser confocal fluorescence microscopy: the rats with SPIO-labeled green fluorescent protein (GFP) transgenic fluorescence were extracted BMSCs, followed by DAPI nuclear staining, then the cell morphology and structure were observed under laser confocal fluorescence microscope.

Osteogenetic induction of BMSCs

BMSCs from the 4th-generation SPIO-labeling group (25 μg Fe/mL) and the unlabeled group were seeded into 6-well plates with 5000 cells/cm^2, when the cells were 70% fused, replaced

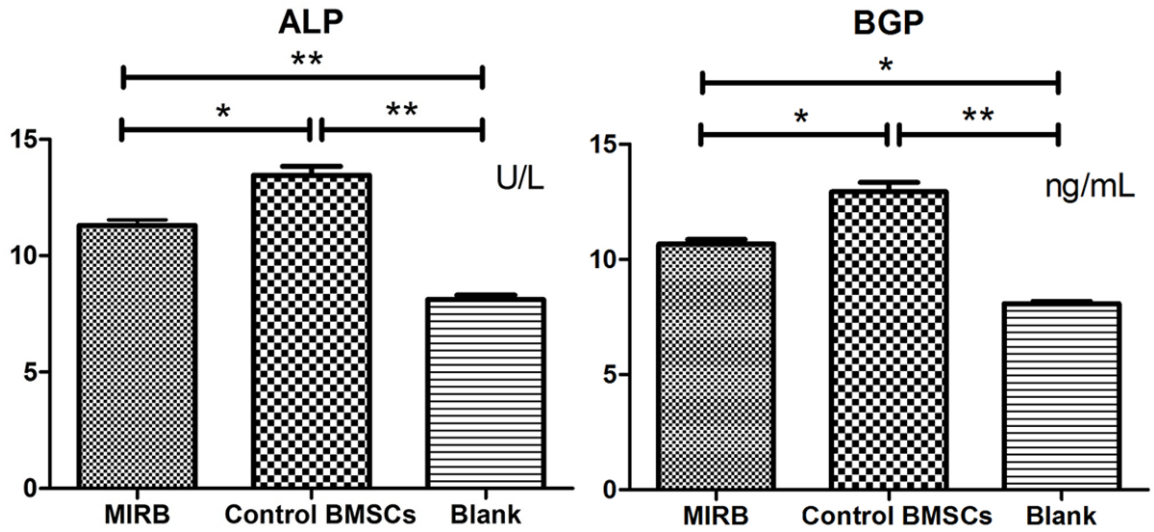

Figure 7. ALP and BGP activity detection by poly-biochemical analyzer. *P<0.05; **P<0.01.

the Gibco osteogenetic differentiation-inducing culture medium, and the medium was changed every three days. 14 days later, the alkaline phosphatase staining kit (Sigma, St. Louis, MO, USA) was used to detect alkaline phosphatase (ALP), and 21 days later, the 1% alizarin red staining (Sigma, St. Louis, MO, USA) was performed to detect the Ca nodules.

Real time -polymerase chain reaction (RT-PCR)

The 25 μg Fe/mL group and the control group were performed the osteogenetic induction, respectively, the cells were collected 7 days later to test the expressions of important osteogenesis-related genes, including bone sialoprotein, ALP, RUNX2, bonemorphogeneticprotein-2 (BMP-2), type 1 collagen (COL-1) and type 3 collagen (COL-3), through analyzing the gene expression, the impacts of SPIO-labeling on osteogenetic capacities of BMSC were then evaluated.

Activity detection of osteocalcin and ALP

The 25 μg Fe/mL group and the control group were performed the osteogenetic induction, respectively, the induction solutions in both groups were discarded 14 days later, and added 10% FBS-containing DMEM/F12 (1:1) medium (without phenol red) for more 48 h cultivation, then collected the culture solutions in the 6-well plates for the quantitative detection of osteocalcin and ALP levels by poly-biochemical analyzer.

Data analysis

The GraphPad Prism 5.0 software (GraphPad, Inc., La Jolla, CA, USA) was used to analyze the experimental data; the data were expressed as mean ± standard error; the Two-way ANOVA was performed to compare the intergroup difference at different time points and among different-level groups; the One-way ANOVA was performed for the intergroup comparison, the test level was set as $\alpha<0.05$.

Results

Culture, morphologic observation and identification of BMSCs

The whole bone marrow wall-adherence method was performed to inoculate BMSCs, a large number of round hematopoietic cells could be seen suspending inside the medium 24 h later, the wall-adherent cells were polygonal and fusiform, gathered together, formed spiral about one week later, arranged radially and covered the flask dishes. The suspended cells were gradually reduced with culture medium changing and passaging, indicating that the 4th-generation suspended cells had basically disappeared. The flow cytometry was then performed to test the surface markers of 4th-generation cells, namely CD90 (98.83%), CD11b (0.36%), CD45 (99.28%) and CD29 (0.3%). The induction experiment showed that the wall-adherent cells had the abilities of osteogenesis and adipogenic differentiation (**Figure 1**).

Detection of cellular viability of MIRB-labeled BMSCs

In CCK-8 experiment, it was found by drawing the histogram of cell proliferation that different-concentration groups and the control group exhibited differences in proliferation on post-labeling 1st, 2nd, 3rd and 4th day, indicating that the concentration under 100 μg Fe/mL would not affect the cellular viabilities of BMSCs (**Figure 2**).

Morphological observation of MIRB-labeled cells

Under TEM, the ultrastructures of SPIO-labeled BMSCs were clear, and the morphology was good. There appeared a large number of particles with high electron densities inside the cytoplasm, which distributed as small lumps or spots, the particles agglomerated, dense and deeply stained, the particle sizes ranged from several tens of nanometers to several hundreds of nanometers, the shapes were irregular, and mainly located inside the cytoplasm, and nearby the smooth endoplasmic reticulum. No particles existed inside the nuclei and the endoplasmic reticulum (**Figure 3**).

SEM showed that the cytoplasm extended the pseudopodia and crawled along the flask wall, the cellular microfilaments and microtubules were clear. There existed different-sized spherical particles distributing around the nuclei, and the SPIO particles near nuclei were as larger as up to hundreds of nanometers, the particles that were far away from the nuclei and in the cytoplasm were smaller, the most were below 100 nanometers. The spectral analysis showed the regions with particles had higher contents of iron (**Figure 3**).

The Prussian blue staining showed that under 25 μg Fe/mL concentration-labeling, the mesenchymal stem cells were spindle and spread, the numbers of cells were counted randomly from five different vision fields, the labeling rate reached 99%. The blue-stained iron particles distributed in the cytoplasm surrounding the nuclei (**Figure 4A**).

The laser confocal microscopy revealed that BMSCs extracted from SPIO-labeled GFP transgenic fluorescent SD rats showed the fluorescent SPIO particles gathering around the nuclei, which were also scattered in the cytoplasm, and the fluorescence intensities gradually descended from nuclei to the surrounding area of plasma membrane. The results were consistent with the results of Prussian blue staining and the SPIO particles' distributions in SEM (**Figure 4B**).

RT-PCR

As shown in **Figure 5**, after the mesenchymal stem cells were performed the osteogenetic induction for 7 days, the expressions of osteogenesis-related genes in the fluorescent SPIO-labeling group showed different degrees of reduction, among which osteopontin, ALP, BMP-2, RUNX2 and bone sialoprotein showed statistical significance ($P<0.05$), while those of COL-1 and COL-3 genes between the MIRB-labeling group and the control groups had no difference.

Identification of ALP and Alizarin Red staining

14 days after SPIO-labeled induction, ALP (Sigma Co) was used for staining (**Figure 6A**), the optical microscope showed positive blue regions of a large number of alkaline phosphatases. 21 days after induction, the Alizarin Red staining showed the deposit of Ca nodules. The corresponding regions observed under a fluorescence microscope showed the distribution of SPIO red fluorescence (**Figure 6B**).

Detection of ALP and osteocalcin by poly-biochemical analyzer

The poly-biochemical analyzer was used to detect the expressions of ALP and osteocalcin among the groups. The results showed that 14 days after induction, the expressions of ALP and BGP of the SPIO-labeling group were significantly lower than the control group, but significantly higher than the blank group ($P<0.05$ or $P<0.01$) (**Figure 7**).

Discussion

In recent years, the repairing treatment of bone fracture and bone defect had been more focused on transplantation and cell therapy, the pluripotent mesenchymal stem cells combined with biological scaffolds were transplanted into the damaged parts, which then proliferated and differentiated into such corresponding functional cells as osteoblasts, myoblasts and neural cells to exert the therapeutic effects [1, 2]. This stem cell transplantation therapy required effectively monitoring the migration

and proliferation of transplanted cells in vivo, MIRB was one fluorescence-coated SPIO reagent recently developed, which had the double-labeled properties of fluorescence and MRI, the fluorescence labeling could accurately visually mark the locations of stem cells, and MRI labeling had the advantage of biological tracing. There still existed the controversy whether the SPIO agent could accurately trace the transplanted stem cells in vivo. Some researchers pointed out that at the beginning of transplantation, the apoptosis of a large number of transplanted cells in vivo existed, while the SPIO particles might be phagocytized by other tissue cells and macrophages, together with the splitting of transplanted cells, thus generating false positive reactions [14-16]. But different studies had shown different points of view, de Vries IJ transplanted the SPIO-labeled dendritic cells into the lymph nodes of patients with melanoma, the SPIO-labeled cells could be detected by MRI, but the histological examination showed that the labeled cells did not express CD68, indicating that they were not macrophages [17]. Mathiasen compared the SPIO-labeled stem cells' injection sites in myocardial infarction model, and found that the border regions of myocardial infarction with implanted SPIO-labeled stem cells occurred less false-positive reactions, while the false-positive reactions occurred more in the situations that the labeled stem cells were directly injected into the infarct areas. The therefore developed fluorescence reporter gene and SPIO double-labeling method were intended to compensate the shortcomings, which was realized by labeling the rhodamine fluorescence-coated MIRB reagent into the stem cells with GFP-fluorescence gene, so it might play the roles of multi-point confirmation by tracing the transplanted stem cells' whereabouts, functional changes and transplantation effects monitoring, adding convincing results, Nan had already demonstrated its feasibility through the MIRB-labeled ADSC [13].

The repairing of stem cell transplantation in the injured tissues was a dynamic process, the environments of injured sites were complex, thus requiring the transplanted stem cells to have the abilities of migration, crawling, proliferating and differentiating into the appropriate functional cells at the injured sites. This required the SPIO-labeled stem cells not only to retain good proliferation and differentiation potentials, but also not to interfere with the movements and migration of normal stem cells. Schafer used Resovist-labeled human bone marrow mesenchymal stem cells and found that the migration and clustering of SPIO-labeled stem cells were impacted, but recovered normal after cultured for two generations [18]. This experiment used rat bone marrow mesenchymal stem cells, and the experiments proved that the application of SPIO labeling concentration less than 100 μg Fe/mL would not significantly affect the proliferation and cell activities, but considering the signal strength of MRI marker and the efficient usage of reagents, 25 μg Fe/mL was the much more appropriate SPIO labeling concentration, consistent with other researchers [10, 13, 19]. SEM results showed that the microfilaments and microtubes of SPIO-labeled cells were clear, the stretch of wall-adherent cells' pseudopodia was normal, and it could be clearly observed that the SPIO particles were concentrated around the nuclei. TEM experiments further showed that the SPIO particles were mainly clustered in the cytoplasm around the nuclei, while did not enter the normal organelles, however we also found that the sizes of intracellular SPIO particles were not uniform, the larger particles could be as large as up to several hundred nanometers, significantly higher than the specifications of SPIO-labeled original solution (35 nm), which gathered around the nuclei, and those in the cytoplasm and far away from the nucle were smaller, indicating that the SPIO particles might occur aggregation around the nuclei after entered the cells, while when the oversized SPIO particles would interfere the normal physiological functions of stem cells still needed further confirmation.

During the osteogenetic experiments, we found that the cells in the SPIO-labeling group could normally induce the expressions of ALP and Ca nodules, suggesting that SPIO-labeled cells had the abilities of osteogenetic differentiation. But through the quantitative analysis by polybiochemical analyzer towards the cellular metabolites, we found that the productions of ALP and osteocalcin by BMSCsin the SPIO-labeling group were decreased. In the RT-PCR gene expression experiments, it was also found that the expressions of osteopontin, ALP, BMP-2, RUNX2 and bone sialoprotein were significantly decreased, suggesting that the fluores-

cent SPIO might downregulate the osteogenesis of mesenchymal stem cells. Currently, there still existed controversy about whether SPIO would affect the osteogenesis of mesenchymal stem cells, some researchers pointed out that SPIO would not affect the osteogenetic properties of BMSCs [9, 20], but most only performed the qualitative analysis, while lacked the comparative quantitative. Rosenberg pointed out after SPIO-labeling, the expressions of Runx-2 and Osterix were not changed [21]. Alicia studied osteogenesis-related gene expressions, the results showed that the SPIO-labeling might downregulate the expressions of some osteogenesis-related genes, consistent with the results of this study [22, 23]. The different results might be caused by the different materials and SPIO labeling methods used by these researchers. According to our SEM results, the SPIO particles gathering around the nuclei could be up to several hundred nanometers, which could interfere with the normal expressions of certain genes. But we also noticed that it was a complex process for stem cells to play their bone repairing roles, and could not determine their osteogenetic abilities simply through analyzing the expressions of specific genes, and the in vivo environments were much more complex, significantly different from the in vitro cell culture conditions. Therefore, the impacts of SPIO-labeling on BMSCs' osteogenetic capabilities still needed further confirmation by in vivo experiment, and the combination of fluorescent MIRB magnetical labeling and GFP-fluorescent BMSCs would be essential to correctly trace the transplanted stem cells and exclude the false-positive reactions generated by in vivo transplantation of SPIO particles.

Conclusions

This study used multiple methods to investigate the biological changes of fluorescent SPIO-labeled BMSCs from many aspects, and proved that 25 μg Fe/mL fluorescent SPIO-labeling would not affect the normal proliferation of BMSCs, the changes of cytoskeletal structures were not obvious, but we found the larger SPIO particles aggregated around the nuclei, and the labeling might downregulate some osteogenetic capabilities of BMSCs, if applied to tracing the bone defect repairing, it still needed further in vivo study for the confirmation.

Acknowledgements

Shenyang Municipal Science and Technology Bureau, Item No: F12-193-9-30. Helps from Researcher Jinmin Liu, Department of transmission electron microscope, Institute of Metal Research, Chinese Academy Science, as well as from the department of Clinical Laboratory, Affiliated Shengjing Hospital, Chinese Medical University.

Disclosure of conflict of interest

None.

Address correspondence to: Weixian Liu, Department of Oral and Maxillofacial Surgery, Shengjing Hospital of China Medical University, 36# Sanhao Street Heping District, Shengyang 110004, Liaoning Province, China. Tel: +86 24 23892617; Fax: +86 24 23892617; E-mail: weixianliucn@126.com

References

[1] Boeckel DG, Shinkai RS, Grossi ML and Teixeira ER. Cell culture-based tissue engineering as an alternative to bone grafts in implant dentistry: a literature review. J Oral Implantol 2012; 38: 538-545.

[2] Patterson TE, Kumagai K, Griffith L and Muschler GF. Cellular strategies for enhancement of fracture repair. J Bone Joint Surg Am 2008; 90: 111-119.

[3] Tang KX, Shen YF, Yang XB, Gu HM, Duan HJ, Yan ZX and Weng JP. A study of tracking the superparamagnetic iron oxide and enhanced green fluorescent protein labeled miniature porcine bone marrow stem cells by in vitro MRI. Zhonghua Nei Ke Za Zhi 2011; 50: 322-327.

[4] Guenoun J, Ruggiero A, Doeswijk G, Janssens RC, Koning GA, Kotek G, Krestin GP and Bernsen MR. In vivo quantitative assessment of cell viability of gadolinium or iron-labeled cells using MRI and bioluminescence imaging. Contrast Media Mol Imaging 2013; 8: 165-174.

[5] Zhang WY, Ebert AD, Narula J and Wu JC. Imaging cardiac stem cell therapy: translations to human clinical studies. J Cardiovasc Transl Res 2011; 4: 514-522.

[6] Mathiasen AB, Hansen L, Friis T, Thomsen C, Bhakoo K and Kastrup J. Optimal labeling dose, labeling time, and magnetic resonance imaging detection limits of ultrasmall superparamagnetic iron-oxide nanoparticle labeled mesenchymal stromal cells. Stem Cells Int 2013; 2013: 353105.

[7] Fan J, Tan Y, Jie L, Wu X, Yu R and Zhang M. Biological activity and magnetic resonance imaging of superparamagnetic iron oxide nanoparticles-labeled adipose-derived stem cells. Stem Cell Res Ther 2013; 4: 44.

[8] Cromer Berman SM, Walczak P and Bulte JW. Tracking stem cells using magnetic nanoparticles. Wiley Interdiscip Rev Nanomed Nanobiotechnol 2011; 3: 343-355.

[9] Jin X, Yang L, Zhang S, Dun X, Wang F and Tan H. Effects of superparamagnetic iron-oxide particles-labeling on the multi-diffentiation of rabbit marrow mesenchymal stem cell in vitro. Sheng Wu Yi Xue Gong Cheng Xue Za Zhi 2012; 29: 125-133.

[10] Addicott B, Willman M, Rodriguez J, Padgett K, Han D, Berman D, Hare JM and Kenyon NS. Mesenchymal stem cell labeling and in vitro MR characterization at 1.5 T of new SPIO contrast agent: Molday ION Rhodamine-B™. Contrast Media Mol Imaging 2011; 6: 7-18.

[11] Song M, Moon WK, Kim Y, Lim D, Song IC and Yoon BW. Labeling efficacy of superparamagnetic iron oxide nanoparticles to human neural stem cells: comparison of ferumoxides, monocrystalline iron oxide, cross-linked iron oxide (CLIO)-NH2 and tat-CLIO. Korean J Radiol 2007; 8: 365-371.

[12] Peng C, Yang K, Xiang P, Zhang C, Zou L, Wu X, Gao Y, Kang Z, He K, Liu J, Cheng M, Wang J and Chen L. Effect of transplantation with autologous bone marrow stem cells on acute myocardial infarction. Int J Cardiol 2013; 162: 158-165.

[13] Nan H, Huang J, Li H, Li Q and Liu D. Assessment of biological characteristics of adipose tissue-derived stem cells co-labeled with Molday ION Rhodamine B™ and green fluorescent protein in vitro. Mol Med Rep 2013; 8: 1446-1452.

[14] Silva AK, Wilhelm C, Kolosnjaj-Tabi J, Luciani N and Gazeau F. Cellular transfer of magnetic nanoparticles via cell microvesicles: impact on cell tracking by magnetic resonance imaging. Pharm Res 2012; 29: 1392-1403.

[15] Terrovitis J, Stuber M, Youssef A, Preece S, Leppo M, Kizana E, Schär M, Gerstenblith G, Weiss RG, Marbán E and Abraham MR. Magnetic resonance imaging overestimates ferumoxide-labeled stem cell survival after transplantation in the heart. Circulation 2008; 117: 1555-1562.

[16] Luciani N, Wilhelm C and Gazeau F. The role of cell-released microvesicles in the intercellular transfer of magnetic nanoparticles in the monocyte/macrophage system. Biomaterials 2010; 31: 7061-7069.

[17] de Vries IJ, Lesterhuis WJ, Barentsz JO, Verdijk P, van Krieken JH, Boerman OC, Oyen WJ, Bonenkamp JJ, Boezeman JB, Adema GJ, Bulte JW, Scheenen TW, Punt CJ, Heerschap A and Figdor CG. Magnetic resonance tracking of dendritic cells in melanoma patients for monitoring of cellular therapy. Nat Biotechnol 2005; 23: 1407-1413.

[18] Schäfer R, Kehlbach R, Müller M, Bantleon R, Kluba T, Ayturan M, Siegel G, Wolburg H, Northoff H, Dietz K, Claussen CD and Wiskirchen J. Labeling of human mesenchymal stromal cells with superparamagnetic iron oxide leads to a decrease in migration capacity and colony formation ability. Cytotherapy 2009; 11: 68-78.

[19] Lu X, Nie Y, Zhao Z, He X, Liu Y, Pulati T and Wu J. SPIO-labeled rat bone marrow mesenchymal stem cells: alterations of biological activity and labeling efficiency assay in vitro. Sheng Wu Yi Xue Gong Cheng Xue Za Zhi 2014; 31: 365-372.

[20] He T, Wang Y, Xiang J and Zhang H. In vivo tracking of novel SPIO-Molday ION rhodamine-B-labeled human bone marrow-derived mesenchymal stem cells after lentivirus-mediated COX-2 silencing: a preliminary study. Curr Gene Ther 2014; 14: 136-145.

[21] Rosenberg JT, Sellgren KL, Sachi-Kocher A, Calixto Bejarano F, Baird MA, Davidson MW, Ma T and Grant SC. Magnetic resonance contrast and biological effects of intracellular superparamagnetic iron oxides on human mesenchymal stem cells with long-term culture and hypoxic exposure. Cytotherapy 2013; 15: 307-22.

[22] El Haj AJ, Glossop JR, Sura HS, Lees MR, Hu B, Wolbank S, van Griensven M, Redl H and Dobson J. An in vitro model of mesenchymal stem cell targeting using magnetic particle labelling. J Tissue Eng Regen Med 2015; 9: 724-33.

[23] Chen YC, Hsiao JK, Liu HM, Lai IY, Yao M, Hsu SC, Ko BS, Chen YC, Yang CS and Huang DM. The inhibitory effect of superparamagnetic iron oxide nanoparticle (Ferucarbotran) on osteogenic differentiation and its signaling mechanism in human mesenchymal stem cells. Toxicol Appl Pharmacol 2010; 245: 272-279.